Direct Measurement of the Strength of Single Ionic Bonds between Hydrated Charges

Evan Spruijt,* Sebastiaan A. van den Berg, Martien A. Cohen Stuart, and Jasper van der Gucht

Laboratory of Physical Chemistry and Colloid Science, Wageningen University, Dreijenplein 6, 6703 HB Wageningen, The Netherlands

ABSTRACT

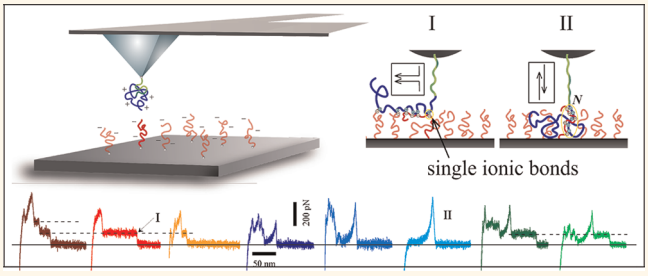

The strength of ionic bonds is essentially unknown, despite their widespread occurrence in natural and man-made assemblies. Here, we use single-molecule force spectroscopy to measure their strength directly. We disrupt a complex between two oppositely charged polyelectrolyte chains and find two modes of rupture: one ionic bond at a time, or cooperative rupture of many bonds at once. For both modes, disruption of the ionic bonds can be described quantitatively as an activated process. The height of the energy barrier is not only lowered by added salt, but also by the applied force. We extract unperturbed ionic bond lifetimes that range from milliseconds for single ionic bonds at high salt concentration to tens of years for small complexes of five ionic bonds at low salt concentration.

KEYWORDS: single molecule force spectroscopy · AFM · ionic bond · electrostatics · polyelectrolyte · polyelectrolyte complex · complex coacervate

Ionic bonds play a key role in many natural macromolecular assemblies. They facilitate DNA compaction,[1,2] they contribute to the extreme stability of enzymes in thermophilic bacteria,[3] and they determine the strength of many bioadhesives.[4] Because of their strength and tunability, ionic bonds see a growing interest for use in man-made responsive materials,[5,6] nanostructures,[7−10] and photovoltaic devices.[11] For ions in a vacuum, Coulomb's Law gives a precise value of the force, but the presence of a medium such as water containing salt ions leads to hydration, dielectric effects, and screening of the charges. How the combination of these effects modifies the short-range attractive force—commonly called "ionic bond"—is still poorly understood. As a result, the strength of ionic bonds between opposite hydrated charges is essentially unknown, making predictions of their stabilizing effect in charge-driven materials impossible.

Here, we use atomic force microscopy (AFM) to directly measure the strength of single ionic bonds. AFM has proved to be a successful method for measuring the strength and rupture dynamics of single covalent,[12] hydrogen,[13] metal−ligand coordination[14] and antibody−antigen[15] bonds. In all single molecule force measurements, the sample molecules are covalently bound to AFM cantilevers *via* a polymeric linker molecule.[12−16] The polymeric linker not only separates the rupture of the investigated complex from contact adhesion of the tip to the substrate, it also exhibits a well-defined relation between extension and the applied force prior to the eventual complex rupture, from which the single molecule origin of the measured force can be established.[16]

RESULTS AND DISCUSSION

Single Molecule Interactions between Oppositely Charged Polyelectrolytes. To assess the strength of ionic bonds between single molecules by AFM, we covalently attach a cationic diblock copolymer (poly(*N*-methyl-2-vinylpyridinium iodide)-*block*-poly(ethylene oxide), $PM2VP_{249}$-*b*-PEO_{134}) to a silicon nitride AFM cantilever, following an adapted method of Hinterdorfer *et al.*[16] The polymer is covalently bound to the AFM tip with its PEO-end, which acts as a neutral, flexible linker, while the PM2VP block is positively charged. We then bring this cantilever in contact with a substrate on which an anionic poly(3-sulfopropyl methacrylate) brush ($PSPMA_{40}$) is grown, according to a previously described and calibrated procedure.[17,18] Upon contact, the oppositely charged polyelectrolytes form complexes consisting of one or multiple ionic bonds. We measure the strength of these bonds in aqueous solutions

* Address correspondence to evan.spruijt@wur.nl.

Received for review March 13, 2012 and accepted May 4, 2012.

Published online May 04, 2012
10.1021/nn301097y

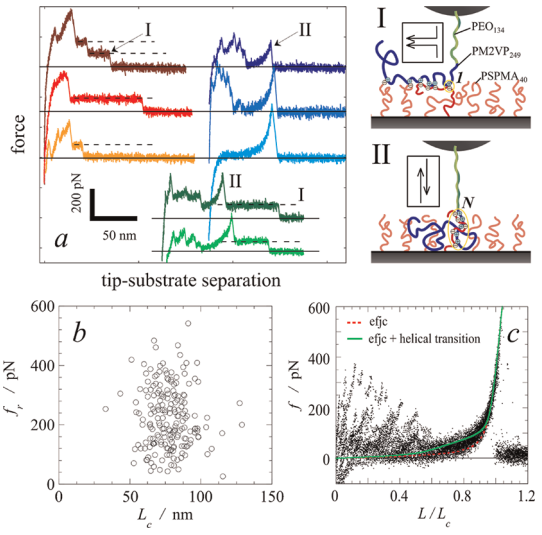

Figure 1. Disruption of ionic bonds between a single polycation and a polyanionic brush measured by AFM. (a) Tip retract curves show disruption of a zipper of ionic bonds, one at a time (I) and simultaneous disruption of cooperative complexes with multiple bonds (II). These curves are measured for the same tip−substrate combination at 1.0 M salt. (b) Distribution of rupture forces and contour lengths of 200 type II events at 1.0 M salt. (c) Rescaled overlay of 30 F−D curves with a type II event and fits to the extensible freely jointed chain (EFJC) model (dotted line) and the EFJC model with a helical to planar transition of the PEO block (solid line).[19]

at various salt concentrations. The overall fraction of force−distance (F−D) curves in which we find an attractive interaction outside the region of contact adhesion (closer than 30 nm) is 16 ± 5% for all conditions. When we repeat experiments with tips without any modification or with only physically adsorbed polymers, we find such interactions in <0.2% of all F−D curves. Figure 1a shows some examples of force curves for a salt concentration of 1.0 M. The measured interactions due to polyelectrolytes come in two characteristic types.

In 8.5 ± 2% of all F−D curves we find a constant force plateau (type I). Neither the frequency of these events, nor the plateau height changes significantly in the first 1000 F−D curves, indicating that no brush erosion takes place. Similar plateau regions in other polymeric systems have been observed for the detachment of polymers adsorbed to a solid surface,[20−22] and for the unzipping of complementary DNA strands.[23] They were attributed to the continuous disruption of successive bonds, one by one, in a zipper-like fashion. In our case, we expect to find such a zipper-like disruption of single bonds when the polymer on the AFM tip binds to an oppositely charged polymer in the brush in a parallel fashion as depicted in Figure 1a-I. Alternatively, the polymer on the tip may form single ionic bonds with several brush polymer chains, as if it was adsorbed on top of the brush. When the tip is retracted, the linker is stretched and a force is exerted on the first ionic bond. Upon failure, partial relaxation of the stretched polymer occurs and only part of the built-up load is transferred to the next ionic bond.[24] This bond in turn breaks at a similar load, resulting in a plateau of constant force during separation.

Another 8 ± 3% of all F−D curves display a characteristic polymer stretching before a rupture event (type II). These rupture forces are typically much larger than the rupture forces of type I events at the same salt concentration. This must mean that rupture involves multiple ionic bonds between the same two polymers, in such a way that the applied force is shared between the bonds: a shear alignment of antiparallel polymer chains (see Figure 1a-II). This clear distinction between parallel and antiparallel orientations is well-known for DNA and β-sheets in proteins; the significant difference in rupture force can in fact be used to selectively deposit DNA onto a surface.[25] In our experiments, combinations of modes I and II are possible, since part of the long polymer on the AFM tip can bind antiparallel to a brush polymer chain (II), while another part can bind a second brush polymer in a parallel fashion (I). Indeed, we find both modes combined in about 1% of all curves (Figure 1a).

We have attributed both rupture modes to interactions of single polymers with the brush on the substrate. Indeed, the sharpness of the tip (R_{tip} = 20 nm) and the low surface coverage obtained using our modification method make it very unlikely that two polymers have exactly the same pull-off distance.[16] Occasionally we find a force curve with two separated rupture events or a multistep desorption (0.5−0.7% of all curves, see Supporting Information), but these are not used in our analysis. Further evidence for the single-molecule nature of the rupture evidence comes from analyzing the polymer stretching curves that precede type II rupture. All curves could be fitted to an extensible freely jointed chain (EFJC) model that includes the force-induced helical-to-planar transition characteristic for PEO,[19] with fit parameters (Kuhn length b = 0.7 ± 0.1 nm, contour length L_c = 78 ± 15 nm, and segment elasticity k_s = 10 ± 2.9 nN/nm) that are consistent with single PEO chains in water (Figure 1c).[19,26] Moreover, the distribution of the contour lengths and rupture forces show no sign of interactions of multiple polymers (Figure 1b).

Effect of Salt on the Interaction Forces. If the rupture events shown in Figure 1a indeed correspond to the breaking of ionic bonds between the oppositely charged polyelectrolytes, then their magnitude should be highly sensitive to the concentration of added salt. In experiments on complex formation of the same polyelectrolytes ($PM2VP_{88}$ and $PSPMA_{96}$) in bulk solutions, we find that the driving force for complexation decreases with increasing salt concentration and vanishes completely above a critical salt concentration of 1.4 ± 0.10 M (NaCl), in agreement with previous observations on complex coacervate formation.[27]

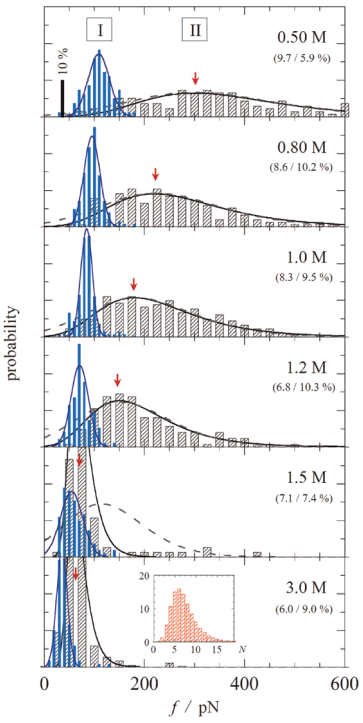

Figure 2. Histograms of type I and II ionic bond rupture forces at various salt concentrations. For each histogram at least 1200 F–D curves are analyzed. The percentages indicate the fraction of rupture events (I/II). Solid lines are Gaussian (type I) and Gumbel (type II) fits of the data. Dashed lines are model predictions of the distribution of type II rupture forces by eq 6. Above the critical salt concentration the model and Gumbel fits mostly overlap. The arrows indicate the most probable rupture force of type II rupture events. The inset shows the Gumbel probability distribution of the number of ionic bonds in a type II complex we used in our model for the force distribution data of type II rupture events.

Indeed, the rupture forces of both type I and II events decrease with increasing salt concentration, as shown in Figure 2. The critical point is reflected by a sudden jump to a lower mean rupture force between 1.2 and 1.5 M for both types of events, after which the mean rupture force remains approximately constant up to 3.0 M. The nonzero residual rupture force beyond 1.5 M salt is attributed to nonelectrostatic interactions between the two types of polymers that do not depend on salt concentration. Finally, reference measurements with either bare tips or bare substrates (see Supporting Information) further support our conclusion that the rupture events shown in Figure 1a correspond to the breaking of ionic bonds between the two polyelectrolytes.

Molecular Rupture Model for Ionic Bonds. For a quantitative understanding of the ionic bond rupture processes in Figure 1, we consider the energy landscape of the disruption of an ionic bond (Figure 3a). When no external force is applied, the energy barrier can be estimated as the difference between the effective electrostatic energy of an ion pair in contact (E_{el}) and the energy of the separated polymeric chains, where

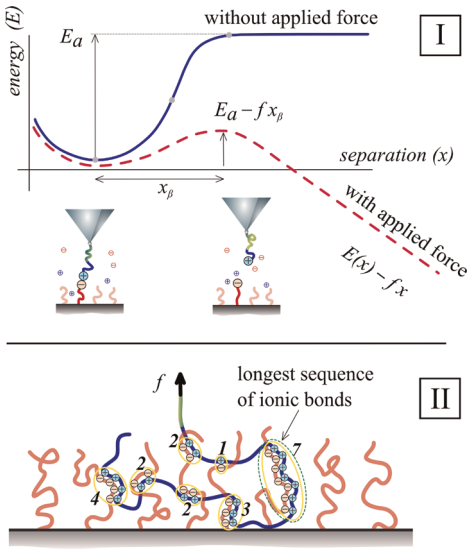

Figure 3. (top) Schematic energy landscape of the disruption of an ionic bond. (bottom) When complexes of multiple ionic bonds are disrupted, the longest sequence of ionic bonds determines the maximum rupture force.

both ionic groups are surrounded by salt (E_{corr}). For the latter we use a Debye–Hückel approximation,[28]

$$\frac{E_a}{k_B T} = -\kappa \ell_B + \frac{\ell_B}{d} = -a\sqrt{c_{salt}} + b \qquad (1)$$

where d is the contact distance of the charged groups in an ion pair, which is of the order of a few Å,[29] $\ell_B = e^2/4\pi\varepsilon_r\varepsilon_0 k_B T$ is the Bjerrum length, which is 7.1 Å in pure water, and κ is the inverse Debye length, which depends on the salt concentration ($\kappa^2 = 8 \times 10^3 \pi N_A \ell_B c_{salt}$ for a 1:1 electrolyte, with concentration c_{salt} in mol/L). The parameters a and b follow from rearrangement and are temperature-dependent constants: $a = (8 \times 10^3 \pi N_A \ell_B^3)^{1/2}$ and $b = \ell_B/d$. We note that the Debye–Hückel approximation assumes that ions are point charges in a continuum dielectric, whereas we use high salt concentrations to study the rupture of ionic bonds, where these assumptions may not be entirely valid. Nevertheless, we have previously found that this simple expression adequately describes the effect of competition between monovalent salt ions and polymeric charges in complexes between oppositely charged polyelectrolytes.[30] Therefore, we apply it here to the forced rupture of ionic bonds.

When an external force is applied, the energy landscape is distorted (Figure 3a). This leads to a lowering of the energy barrier and an enhancement of the dissociation rate.[31] For a single rupture process,

$$k(f) = \omega_0 g(f) \exp\left(\frac{E_a - f x_\beta}{k_B T}\right) = k_0 g(f) e^{f/f_\beta} \qquad (2)$$

where k is the dissociation rate, k_0 the dissociation rate in the absence of force ($k_0 = \omega_0 \exp(-E_a/k_B T)$), x_β is the distance from the energy minimum to the transition state (see Figure 3a) and $f_\beta = k_B T/x_\beta$. If the energy

barrier is sharp, an applied force mainly alters the barrier height and $g(f) \approx 1$. In an AFM experiment with a constant loading rate ($f = r_f t$), the probability of bond rupture at a given force can be found from the product of the rupture probability at that force and the survival probability up to that force.

$$p(f) = \frac{1}{r_f} k(f) \exp\left[-\int_0^f \frac{1}{r_f} k(f')\, df' \right]$$
$$\approx \frac{k_0}{r_f} e^{f/f_\beta} \exp\left[\frac{k_0 f_\beta}{r_f} (1 - e^{f/f_\beta}) \right] \quad (3)$$

For the rupture process described by eq 2, this leads to a characteristic probability distribution with a maximum at $f^* = f_\beta \ln(r_f/f_\beta k_0)$, assuming a constant loading rate.[32] A combination of eqs 1 and 2 provides a prediction for the effect of salt on the mean rupture force of a single ionic bond.

$$f^* = f_\beta \ln\left(\frac{r_f}{\omega_0 f_\beta}\right) - f_\beta a \sqrt{c_{salt}} + f_\beta b \quad (4)$$

In a complex with multiple ionic bonds (Figure 1a-I and II), the relevant energy barrier and the effect of loading depend on the way one applies the force to the complex. As argued above, in the case of polyelectrolyte chains, the bonding groups are located along a polymer backbone, and we have two ways of loading the ionic bonds: as a zipper (parallel, Figure 1a-I) and in shear (antiparallel, Figure 1a-II).[24]

In the case of zipper-like disruption, the relevant energy barrier is that of a single ionic bond. The plateau we measure is the average force of many stochastic single bond rupture events, each following eq 3. A distribution of the plateau force is therefore expected to be Gaussian, as shown in Figure 2. The width of the corresponding energy barrier can be otained from a plot of the most probable force *versus* ln *v*, where $v = r_f/k_s$ is the average tip velocity. We find that f_β does not depend strongly on salt concentration, varying from 26 pN at 1.0 M salt to 30 pN at 0.5 M salt (see Supporting Information). Consequently, $x_\beta = 0.144$ nm, which is similar to the barrier width of hydrogen bond rupture[13] and is in good agreement with the dimensions of the ionic groups on the polymer chains. Using this value for x_β, we can use eq 4 to describe the effect of salt on the strength of single ionic bonds, as shown in Figure 4. We find that $a = 4.5 \pm 0.5\ M^{-0.5}$ and $B = f_\beta \ln(r_f/\omega_0) f_\beta) + f_\beta b = 170 \pm 10$ pN, corresponding to an effective dielectric constant of $\varepsilon_r = 53$ at $T = 293$ K, which is quite reasonable for a local ionic strength near the complex of 1−2 M.[33] If we assume the ionic bond distance, *d*, to be 0.2 ± 0.03 nm, that is, slightly larger than typical covalent N−O bond lengths, and independent of salt concentration,[34] we find that the energy barrier varies from 6 k_BT in salt-free aqueous solutions to 1 k_BT around the critical salt concentration (see inset in Figure 4). These values are in good agreement with the computed energies for salt bridges occurring in proteins.[29]

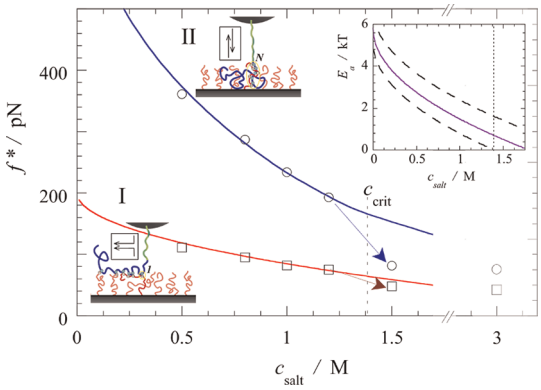

Figure 4. Experimental (symbols) and theoretical (lines) mean rupture forces for single ionic bonds (type I) and complexes of multiple ionic bonds (type II) as a function of salt concentration, measured at a tip velocity of 500 nm/s (approximate loading rate at rupture 3×10^3 pN/s). Close to the critical salt concentration (c_{crit}) we experimentally find a jump to lower forces and the model breaks down. The inset shows the predicted energy barrier for single ionic bond rupture.

Disruption of multiple (*N*) ionic bonds in a shear arrangement (Figure 1a-II) requires much larger forces than disruption of a zipper of ionic bonds, because the force is shared between all *N* bonds. The complex is expected to fail at a force f_N^* where $\partial \ln p(f)/\partial f = 0$, which leads to an implicit relation for f_N^*[24]

$$k_{N\to 0}(f) = \left[\sum_{n=1}^{N} \frac{1}{n k_0} \exp\left(-\frac{f}{n f_\beta} \right) \right]^{-1} \quad (5)$$

$$f_N^* = N f_\beta \ln\left(\frac{r_f}{k_0 f_N^*}\right)$$
$$= N f_\beta \ln\left(\frac{r_f}{\omega_0 f_N^*}\right) - aN f_\beta \sqrt{c_{salt}} + bN f_\beta \quad (6)$$

Further evidence for the proposed shear arrangement in type II events comes from the nonlinear relation between f^* and ln r_f, which we observe experimentally (see Supporting Information). Before analyzing the data, we note that an additional complication in the disruption of polyelectrolyte complexes is that the number of ionic bonds (*N*) formed when the tip-bound polymer penetrates into the brush is not constant, but can vary. Sequences of ion pairs alternate with more loosely arranged parts of the chain (see Figure 3b). We presume that the maximum rupture force measured in experiments is determined by the longest sequence of consecutive ion pairs. For a given probability of ion pair formation, the probability distribution of this longest sequence converges to the same distribution as the longest run of heads in a series of coin flips: a Gumbel extreme value distribution, with a tail at large *N*.[35] We can now verify our ionic bond rupture model in eqs 1, 3,

and 5 for the disruption of cooperative complexes of ionic bonds. Since type II events are measured in the same series as type I events, the values of x_β, a, and b should not change. Indeed, we find excellent agreement between our experimentally measured rupture force distributions of type II events and the theoretical predictions, as shown in Figure 2. The longest sequence of ionic bonds is given by the Gumbel distribution shown in the inset of Figure 2 (full expression in Supporting Information) and the rupture force distributions themselves can be approximated by a Gumbel distribution. The mean rupture forces decrease more strongly with increasing salt concentration than in the case of single ionic bonds, as predicted by our model (see Figure 4). Just like for single ionic bonds, our model breaks down close to the critical salt concentration, where the energy barrier per ionic bond becomes of order k_BT.

Single Molecule Interactions with Multilayers. Ionic bonds have a strongly salt-dependent strength and collectively they can become as strong as covalent bonds, even in water. These interactions and rupture mechanisms can play an important role in protein−protein and protein−ligand interactions.[36] However, in nature and in man-made applications using electrostatic complexes, the relevant interactions often occur between charged macromolecules and existing complexes of oppositely charged macromolecules.[5−8,11,37] Our experimental setup can easily be changed to measure such interactions as well. Without changing the tips, we simply increase the number of polyelectrolyte layers on our substrates by subsequently dipping the substrate with PSPMA brushes in 1 g/L solutions of $PM2VP_{88}$ and $PSPMA_{96}$ in 1.0 M NaCl. In this way we create substrates with one (only PSPMA brush), two (PSPMA + PM2VP), three (PSPMA + PM2VP + PSPMA), or more "layers", although complete mixing between the nongrafted polyelectrolytes on the surface is expected at the applied salt concentration. We indeed measure an increase in dry layer thickness from 13 to 16 to 19 nm using ellipsometry. For more than three layers, we find a constant layer thickness of 20 ± 2 nm, consistent with complete mixing of the layers.

Figure 5 shows the force histograms for type II rupture events at 1.0 M NaCl for one, two, and three layers on the substrate. With two or more layers covering the underlying silica, we no longer find type I events, probably because a different rupture process from the one depicted in Figure 3 takes place. Interestingly, the rupture force of the type II rupture events decreases significantly with the number of layers. Moreover, the force distributions become narrower and closer to a Gaussian distribution. For more than three layers, we find no further change in the rupture force distributions. Both effects can be explained by considering the rupture mechanism between a single polyelectrolyte and the substrate. In the case of one

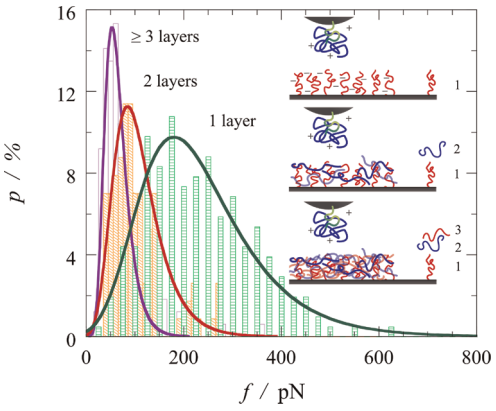

Figure 5. Histograms of rupture forces of a $PM2VP_{249}$ cationic block from a substrate with a varying number of polyelectrolyte "layers" at 1.0 M salt. One layer corresponds to a PSPMA brush only, two layers indicate that free PM2VP is adsorbed into the PSPMA brush, and three layers indicate a second adsorption step with free PSPMA. Solid lines are Gumbel fits to the data.

layer, separation of the tip and the substrate involves rupture of ionic bonds, as discussed above. However, when the substrate is already covered with a stoichiometric polyelectrolyte complex (two layers: PSPMA + PM2VP), there is no longer a strong electrostatic driving force for formation of ionic bonds and either fewer or weaker ionic bonds will be formed between the cationic block copolymer and complex. Moreover, the presence of a complex on the substrate increases the local charge density and thus decreases the activation energy for separation of the ion pairs (see eq 1). Indeed, we find that the distribution resembles that of a higher salt concentration than 1.0 M (see Figure 2). Finally, when the substrate contains three or more layers, also free PSPMA polymers are present that can (partly) neutralize the cationic block copolymer when tip and substrate are separated. Separation now occurs between two neutral complexes, and the energy barrier involved in this process is determined by the interfacial energy of the polyelectrolyte complex. Even for strongly charged polyelectrolytes, these interfacial energies are relatively low.[38] As a result, the rupture forces measured for a substrate with three layers are lower than that for one or two layers; they are even lower than the expected rupture forces for single ionic bonds at the same salt concentration (see Figure 2).

CONCLUSIONS

Ionic bonds are reversible and highly tunable connections. For the *N*-methyl-2-vinylpydidinium/3-sulfopropyl-methacrylate bonds considered here, the strength ranges from roughly 1 k_BT close to the critical salt concentration to over 6 k_BT at low salt concentration. Cooperativity of the ionic bonds further amplifies this difference. As a result, the lifetime of ionic bonds in natural aqueous systems can range from milliseconds for single ionic bonds at high salt concentration to tens

of years for small complexes of five ionic bonds at low salt concentration. This versatility offers many opportunities for use of ionic bonds in new man-made materials. Under the right conditions a small complex of ionic bonds may be stronger than a covalent bond,[12] yet remain completely reversible: it can be "unlocked" at any time by addition of salt.[10] In practical applications, the way charged groups are grafted to scaffolds or surfaces will play an important role in the stability of the complexes they form. When disassembly involves separation of the charges, much higher forces are required than for multilayer assemblies.

METHODS

Materials. We use triangular DNP silicon nitride probes (Bruker). The cantilevers we use for force spectroscopy measurements have a spring constant of $k = 0.06 \pm 0.01$ N/m and a tip radius of 20 nm. Flat silicon wafers with a 3 nm layer of native oxide are purchased from WaferNet. Before surface modification all cantilevers and substrates are cleaned by immersion in piranha solution (70/30 96% H_2SO_4/35% H_2O_2) for 30 min, rinsing thoroughly with Milli-Q water and ethanol and drying under nitrogen.

Tip Modification. The dried cantilevers are modified by reacting in a solution of 2.8 g of 2-aminoethanol hydrochloride in 5 mL of dry dimethylsulfoxide (DMSO) with 4 Å molecular sieves for 16 h. After 16 h, the cantilevers are rinsed with dry DMSO, transferred into a 0.040 M *p*-phenylene-diisocyanate solution in dry DMSO and left to react for no longer than 30 min, to avoid precipitation of solution-polymerized isocyanates onto the cantilever surface. The cantilevers are rinsed once again and transferred to the final solution of 10 g/L hydroxy-EO-terminated poly(*N*-methyl-2-vinylpyridium)-*block*-poly(ethylene oxide), $PM2VP_{249}$-*b*-PEO_{134}−OH (Polymer Source; degree of quaternization, 86%) in dry DMSO and left for 1 h. After 1 h the cantilevers are rinsed thoroughly with Milli-Q water and ethanol, dried under nitrogen, and stored in a gel pack until use.

Substrate Modification. Polyelectrolyte brushes are synthesized by surface-initiated atom transfer radical polymerization (SI-ATRP). We modify 1×1 cm^2 cut silicon wafers by immersion in a 5% (v/v) solution of 3-trimethoxysilylpropyl-2-bromo-2-methylpropionate (Gelest Inc. UK) in hexane for 1 h. After 1 h, the substrates are rinsed with hexane, dried under nitrogen, and transferred to a Schlenk tube under argon atmosphere. The ATRP solution is prepared by dissolving 2.25 g potassium 3-sulfopropylmethacrylate (KSPMA), 25 mg 2,2′-bipyridine, and 3.5 mg of $CuCl_2$ in 1.25 mL of Milli-Q water and 2.50 mL of methanol, degassing by bubbling argon for 10 min and subsequently adding 9.0 mg of CuCl. After bubbling argon for another 5 min, the ATRP solution is transferred to the Schlenk tube using a syringe. The ATRP reaction is quenched after 20 min by opening the tube to oxygen; the substrates are rinsed with Milli-Q water, methanol, and ethanol, dried under nitrogen, and stored until use. All substrates have a dry brush thickness of 13 ± 2 nm (Sentech SE-400 ellipsometer), corresponding to a number average degree of polymerization of $N_{neg} = 40$, at an estimated grafting density of 0.8 ± 0.3 nm^{-2}.[17,18]

Force Spectroscopy Experiments. All force curves are recorded with the Force Robot 300 (JPK), using a small volume liquid cell (70), sealed with a rubber ring at a temperature of $T = 293 \pm 2$. In all experiments the liquid cell is filled with an aqueous solution of NaCl (various concentrations) in Milli-Q water at pH 7 ± 0.5. The cantilevers are calibrated (deflection sensitivity from the slope at $f > 1$ nN, spring constant using the thermal tune method with corrections for nonideality and cantilever support[39]) at 3.0 M NaCl, where the brushes are collapsed and no attraction is recorded. We verify that this procedure yields correct calibration values (difference <2%) from a calibration against bare silica and a brush with and without modification. Typical F−D curves are recorded for an approach range of 500 nm, a tip velocity (v) of 500 nm/s, no surface delay, and a sampling rate of 4 kHz. In every cycle of approach and retract the tip is lowered to a constant load of 1−2 nN. The actual loading rates at rupture are calculated from EFJC fits of the stretching events (see Figure 1a). Every 100 F−D curves, the substrate is moved by 1.2 and the photodiode is realigned. In total 1000−10 000 F−D curves are recorded for every tip−substrate−solvent combination. For every salt concentration, we measure at least two independent tip−substrate combinations. In the analysis we combine the results for different tip−substrate combinations. Because inevitably some physically adsorbed polymers are present on the AFM tips after modification and thorough rinsing, we discard the first 100 F−D curves from our analysis and start collecting the data after moving to a second location on the substrate. We then make a raw selection of all F−D curves using a custom-made Matlab routine, selecting only those curves that exhibit (1) a jump in the force averaged over three subsequent points that is larger than three times the typical variations in averaged force in the baseline, with (2) a location of the jump that is further than 50 nm from the wall (where the force turns repulsive). We then discard the force curves that show interactions originating from two tip-bound polymers. We sort the remaining force curves in two types: curves with a plateau of constant force and curves with a stretching event. All curves with a force standard deviation smaller than 1.1 times the baseline standard deviation over more than 10 nm from the previously established jump in force are automatically classified as plateau. We manually check the classifications to rule out obvious errors. Finally, the selected F−D curves are further analyzed using the JPK data processing software.

Conflict of Interest: The authors declare no competing financial interest.

Acknowledgment. We thank J. Sprakel and H.-J. Butt for discussions. E.S. acknowledges financial support from The Netherlands Organisation for Scientific Research (NWO).

Supporting Information Available: Reference measurements with unmodified tips, bare substrates and substrates with physically adsorbed polymers, force curves with multiple stretching events, rupture force versus loading rate data for both types of events at various salt concentrations, and the expressions for the rupture force of a complex with multiple ionic bonds in an antiparallel arrangement. This material is available free of charge *via* the Internet at http://pubs.acs.org.

REFERENCES AND NOTES

1. Widom, J. Structure, Dynamics and Function of Chromatin *in Vitro*. *Annu. Rev. Biophys. Biomol. Struct.* **1998**, *27*, 285–327.
2. Perico, A.; La Penna, G.; Arcesi, L. Electrostatic Interactions with Histone Tails May Bend Linker DNA in Chromatin. *Biopolymers* **2006**, *81*, 20–28.
3. Perutz, M. F. Electrostatic Effects in Proteins. *Science* **1978**, *201*, 1187–1191.
4. Stewart, R. J.; Wang, C. S.; Shao, H. Complex Coacervates as a Foundation for Synthetic Underwater Adhesives. *Adv. Colloid Interface Sci.* **2011**, *167*, 85–93.
5. Decher, G. Fuzzy Nanoassemblies: Toward Layered Polymeric Multicomposites. *Science* **1997**, *277*, 1232–1237.
6. Lemmers, M.; Sprakel, J.; Voets, I. K.; van der Gucht, J.; Cohen Stuart, M. A. Multiresponsive Reversible Gels Based on Charge-Driven Assembly. *Angew. Chem., Int. Ed.* **2010**, *49*, 708–711.
7. Cohen Stuart, M. A.; Hofs, B.; Voets, I. K.; de Keizer, A. Assembly of Polyelectrolyte-Containing Block Copolymers in Aqueous Media. *Curr. Opin. Colloid Interface Sci.* **2005**, *10*, 30–36.

8. Biesheuvel, P. M.; Mauser, T.; Sukhorukov, G. B.; Möhwald, H. Micromechanical Theory for pH-Dependent Polyelectrolyte Multilayer Capsule Swelling. *Macromolecules* **2006**, *39*, 8480–8486.
9. Capito, R. M.; Azevedo, H. S.; Velichko, Y. S.; Mata, A.; Stupp, S. I. Self-Assembly of Large and Small Molecules into Hierarchically Ordered Sacs and Membranes. *Science* **2008**, *319*, 1812–1816.
10. Spruijt, E.; Bakker, H. E.; Kodger, T. E.; Sprakel, J.; Cohen Stuart, M. A.; van der Gucht, J. Reversible Assembly of Oppositely Charged Hairy Colloids in Water. *Soft Matter* **2011**, *7*, 8281–8290.
11. Lutkenhaus, J. L.; Hammond, P. T. Electrochemically Enabled Polyelectrolyte Multilayer Devices: From Fuel Cells to Sensors. *Soft Matter* **2007**, *3*, 804–806.
12. Grandbois, M.; Beyer, M.; Rief, M.; Clausen-Schaumann, H.; Gaub, H. E. How Strong Is a Covalent Bond? *Science* **1999**, *283*, 1727–1730.
13. Embrechts, A.; Schönherr, H.; Vancso, G. J. Rupture Force of Single Supramolecular Bonds in Associative Polymers by AFM at Fixed Loading Rates. *J. Phys. Chem. B* **2008**, *112*, 7359–7362.
14. Kudera, M.; Eschbaumer, C.; Gaub, H. E.; Schubert, U. S. Analysis of Metallo-Supramolecular Systems Using Single-Molecule Force Spectroscopy. *Adv. Funct. Mater.* **2003**, *13*, 615–620.
15. Hinterdorfer, P.; Baumgartner, W.; Gruber, H. J.; Schilcher, K.; Schindler, H. Detection and Localization of Individual Antibody-Antigen Recognition Events by Atomic Force Microscopy. *Proc. Natl. Acad. Sci. U.S.A.* **1996**, *93*, 3477–3481.
16. Riener, C. K.; Stroh, C. M.; Ebner, A.; Klampfl, C.; Gall, A. A.; Romanin, C.; Lyubchenko, Y. L.; Hinterdorfer, P.; Gruber, H. J. Simple Test System for Single Molecule Recognition Force Microscopy. *Anal. Chim. Acta* **2003**, *479*, 59–75.
17. Ramstedt, M.; Cheng, N.; Azzaroni, O.; Mossialos, D.; Mathieu, H. J.; Huck, W. T. S. Synthesis and Characterization of Poly(3-sulfopropylmethacrylate) Brushes for Potential Antibacterial Applications. *Langmuir* **2007**, *23*, 3314–3321.
18. Spruijt, E.; Cohen Stuart, M. A.; van der Gucht, J. Dynamic Force Spectroscopy of Oppositely Charged Polyelectrolyte Brushes. *Macromolecules* **2010**, *43*, 1543–1550.
19. Oesterhelt, F.; Rief, M.; Gaub, H. E. Single Molecule Force Spectroscopy by AFM Indicates Helical Structure of Poly-(ethylene-glycol) in Water. *New J. Phys.* **1999**, *1*, 6.1–6.11.
20. Hugel, T.; Grosholz, M.; Clausen-Schaumann, H.; Pfau, A.; Gaub, H. E.; Seitz, M. Elasticity of Single Polyelectrolyte Chains and Their Desorption from Solid Supports Studied by AFM Based Single Molecule Force Spectroscopy. *Macromolecules* **2001**, *34*, 1039–1047.
21. Scherer, A.; Zhou, C.; Michaelis, J.; Brauchle, C.; Zumbusch, A. Intermolecular Interactions of Polymer Molecules Determined by Single-Molecule Force Spectroscopy. *Macromolecules* **2005**, *38*, 9821–9825.
22. Sonnenberg, L.; Parvole, J.; Borisov, O.; Billon, L.; Gaub, H. E.; Seitz, M. AFM-Based Single Molecule Force Spectroscopy of End-Grafted Poly(acrylic acid) Monolayers. *Macromolecules* **2006**, *39*, 281–288.
23. Essevaz-Roulet, B.; Bockelmann, U.; Heslot, F. Mechanical Separation of the Complementary Strands of DNA. *Proc. Natl. Acad. Sci. U.S.A.* **1997**, *94*, 11935–11940.
24. Williams, P. M. Analytical Description of Dynamic Force Spectroscopy: Behaviour of Multiple Connections. *Anal. Chim. Acta* **2003**, *479*, 107–115.
25. Kufer, S. K.; Puchner, E. M.; Gumpp, H.; Liedl, T.; Gaub, H. E. Single Molecule Cut-and-Paste Surface Assembly. *Science* **2008**, *319*, 594–596.
26. Zou, S.; Schönherr, H.; Vancso, G. J. Stretching and Rupturing Individual Supramolecular Polymer Chains by AFM. *Angew. Chem., Int. Ed.* **2005**, *44*, 956–959.
27. Spruijt, E.; Westphal, A. H.; Borst, J. W.; Cohen Stuart, M. A.; van der Gucht, J. Binodal Compositions of Polyelectrolyte Complexes. *Macromolecules* **2010**, *43*, 6476–6484.
28. Hill, T. *An Introduction to Statistical Thermodynamics*; Dover Publications: Mineola, NY, 1986.
29. Kumar, S.; Nussinov, R. Relationship between Ion Pair Geometries and Electrostatic Strengths in Proteins. *Biophys. J.* **2002**, *83*, 1595–1612.
30. Spruijt, E.; Sprakel, J.; Lemmers, M.; Cohen Stuart, M. A.; van der Gucht, J. Relaxation Dynamics at Different Time Scales in Electrostatic Complexes: Time−Salt Superposition. *Phys. Rev. Lett.* **2010**, *105*, 208301.
31. Evans, E.; Ritchie, K. Dynamic Strength of Molecular Adhesion Bonds. *Biophys. J.* **1997**, *72*, 1541–1555.
32. Ray, C.; Brown, J. R.; Akhremitchev, B. B. Correction of Systematic Errors in Single-Molecule Force Spectroscopy with Polymeric Tethers by Atomic Force Microscopy. *J. Phys. Chem. B* **2007**, *111*, 1963–1974.
33. Loginova, D. V.; Lileev, A. S.; Lyashchenko, A. K. Dielectric Properties of Aqueous Potassium Chloride Solutions as a Function of Temperature. *Russ. J. Inorg. Chem.* **2002**, *47*, 1426–1433.
34. Israelachvili, J. *Intermolecular & Surface Forces*; Elsevier Academic Press: Waltham, MA, 1991.
35. Gordon, L.; Schilling, M. F.; Waterman, M. S. An Extreme Value Theory for Long Head Runs. *Probab. Theory Relat. Fields* **1986**, *72*, 279–287.
36. Kundrotas, P. J.; Alexov, E. Electrostatic Properties of Protein−Protein Complexes. *Biophys. J.* **2006**, *91*, 1724–1736.
37. de Vries, R. DNA Condensation in Bacteria: Interplay between Macromolecular Crowding and Nucleoid Proteins. *Biochimie* **2010**, *92*, 1715–1721.
38. Spruijt, E.; Sprakel, J.; Cohen Stuart, M. A.; van der Gucht, J. Interfacial Tension between a Complex Coacervate Phase and Its Coexisting Aqueous Phase. *Soft Matter* **2010**, *6*, 172–178.
39. Stark, R. W.; Drobek, T.; Heckel, W. M. Thermomechanical Noise of a Free V-Shaped Cantilever for Atomic-Force Microscopy. *Ultramicroscopy* **2001**, *86*, 207–215.